Original Article

Studies on the Removal of Indigo Carmin from Aqueous Solutions by GO, Oxidized MWCNTs, AC, and MWCNTs

Shahryar Abbasi[1] **Hadi Noorizadeh**[2*]

1. Professor in Chemistry, Department of Chemistry, Faculty of Science, Ilam University, Ilam, Iran
2. PhD student in Chemistry, Department of Chemistry, Faculty of Science, Ilam University, Ilam, Iran

***Correspondence to**: Hadi Noorizadeh
hadinoorizadeh@yahoo.com

(Received: 28 Apr. 2017; Revised: 27 Sept. 2017; Accepted: 8 Jan. 2018)

Abstract

Background and purpose: Quick removal of dye from water and waste water is very important in the research related to eliminating pollutions; this is because of the spread of damaging effects of dyes in water on the human beings and the environment. Four different carbon nanostructures, namely graphene oxide, oxidized multiwalled carbon nanotubes, activated carbon, and multiwalled carbon nanotubes were applied as adsorbents for the removal of Indigo Carmin (IC) dye from aqueous solution.

Materials and Methods: These carbon nanostructures were determined by X-ray diffractometer and scanning electron microscope. Batch adsorption experiments were then performed to investigate the effect of solution pH, concentration, contact time, and temperature on IC removal. To study the characteristics of IC adsorption process, adsorption constants were calculated by first-order and pseudo second-order models.

***Results*:** Adsorption equilibrium was indicated with Freundlich and Langmuir isotherm models. This study was the first research conducted on the removal of dye which uses four carbon nanostructures adsorbents.

***Conclusion*:** The results indicated better efficiency for GO in IC removal than other carbon adsorbents. The isotherm parameters for the Freundlich and Langmuir models were calculated. The kinetics research also revealed that the experimental data was well fitted by pseudo second-order equation.

***Keywords*:** Water pollution; Indigo Carmin; Graphene oxide; Carbon nanotubes; Activate carbon; Adsorption

Citation: Abbasi Sh, **Norizadeh H*.** Studies on the Removal of Indigo Carmin from Aqueous Solutions by GO, Oxidized MWCNTs, AC, and MWCNTs. 2018; 6 (1):9-24

1. Introduction

The dyes in water and waste water are causing major problems for human health and environment due to their harmful effects. Textile industry produces large amounts of waste that overall include large amounts of soluble salts, organic substances, and surfactants significantly in the form of dye molecules. Considering its intricate chemical structure, when released to the environment untreated, dyes are not simply decomposed by bacteria and stay for a long time in ecosystem. Indigo Carmine (IC) dye because of its contaminating effect on the environment is considered as a serious public and environmental problem. Hence, this dye and it scanner-causing properties can be fatal (1, 2).

IC is an anionic dye. In addition, the use of IC can lead to severe damages to human, such as failure of liver, kidney, brain and genital tract. Significant parts of several million tons of dyes are usually drained into water systems contaminating them by dyes. So, it is essential to remove this organic contaminant via a suitable therapy method (3, 4).Several treatment procedures, such as coagulation, oxidative process, electrolysis sedimentation, and adsorption have been proposed for removing dye from effluent.

Among these methods, the adsorption has been found to be very competitive into other processes due to its higher adsorption capacity, lower cost, and efficiency. Multi-absorbent methods are applied to remove dye from water and effluent, such as agro-industrial chitosan, minerals, byproduct, bacterial, and fungal biomass, multiwalled carbon nanotubes (MWCNTs), Oxidized multiwalled carbon nanotubes (Oxidized MWCNTs), activated carbon(AC), and Graphene oxide (GO) (3-6).

Recently, graphene and graphene oxide (GO) are strongly developed to have a unique range of properties. Graphene is a fundamental building block for graphitic materials, and can be turned to other forms of carbon nanostructure. The CNTs functionalized by different reagents that have various degrees of oxidation is a well-known method among functional groups on Oxidized multi-walled carbon nanotubes. Compared with CNTs, GO has the sp^2 hybrid carbon nanostructure and more particular surface area that couldbe achieved from graphite via an easy chemical redox method (7, 8). MWCNTs, Oxidized MWCNTs, AC and GO are newfound carbonaceous nanosized, whose electronic properties and special structures cause them to have robust reactions with organic molecules, through non-covalent forces as intermolecular force, hydrophobic interactions, electrostatic forces, and hydrogen bonding (9, 10).

Their nanoparticle structures also cause some advantages, such as high adsorption capacity, effectiveness in wide pH range, and quick equilibrium rates (11).In the present research, GO, Oxidized MWCNTs, AC, and MWCNTs were applied for the removal of Indigo Carmin (IC) molecules from aqueous solution. Hence, the effects of different parameters were studied. The Freundlich and Langmuir isotherms were also applied to fit the equilibrium data. Finally, the adsorption kinetics was investigated.

2. Materials and methods

2.1. Preparation of carbonaceous materials

The chemical structure and absorption spectrum of IC is shown in Figure 1. The adsorbent materials applied in this study, commercial MWCNTs, and AC were all procured from Merck (Darmstadt, Germany).

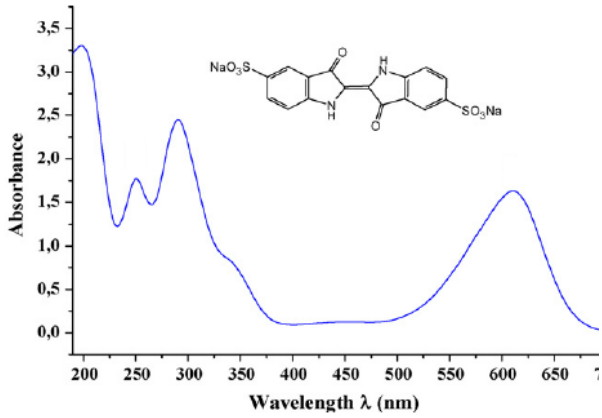

Figure 1. Absorption spectrum and chemical structure of IC

2.2. Oxidation of MWCNTs

MWCNTs with inner diameter 5–15 nm, outer diameter 60–90 nm, length 5–20μm, and purity≥95 were applied. For oxidation, 3 g MWCNTs were put in a 1 L round bottom flask with reflux condenser. Then, 300 mL concentrated nitric acids (65%) were added to it. The blend was then refluxed for 50 h at 120ºC. After that, the mixture was cooled to room temperature, and 500 mL double-distilled water was added. Then excess water is poured and solid to dry it was placed in vacuum-filtered. Wash was duplicated until the water pH got closer to 7, and then it was pursued by drying in vacuum oven at 110ºC (12).The Brunauer–Emmett–Teller (BET) was used toestimate SSAs. A surface area was obtained by theory of BET that measured at 77 K. This is a standard method for computing the SSA of sample (13). The results displayed that the SSAs of oxidized MWCNTs and MWCNTs were 158 and 115m^2g^{-1}, respectively. The Barrett–Johner–Halenda Method was also used for measuring the pore size of oxidized MWCNTs and MWCNTs. The pore volume and average pore diameter were 0.25 cm^3 g^{-1} and 38 nm for oxidized MWCNTs, and 0.18 cm^3g^{-1} and 30 nm for MWCNTs, respectively.

2.3. Preparation of activated carbon

Double distilled water is kept in flacons. Then, carbon is digested on the H_3PO_4 5N solution and heated in 90º C for three hours. Mixture is then cooled, and afterward, it was washed many times with water until soluble impurities are eliminated. The AC is also exposed to air oven at a temperature of 130^{oC} for two hours (14). Then, the BET isotherm is applied; the V_{TOTAL} and S_{BET} were estimated to be 0.065 ml/g and 66.75 m^2/g, respectively. The volume of micropores (V_{mic}) was computed to be 0.015cc/g, and via subtracting the $V_{TOTAL}$from the V_{mic}, the V_{meso} was documented to be 0.048ml/g. In this research, about 71 percent of the total pores volume in the AC was linked to the V_{meso}; so, for the adsorption of adsorbate to molecular dimensions of 25nm and less, the produced AC was found suitable.

2.4. Synthesis of graphene oxide

To apply the modified Hummers Method, graphite oxide (GO) was readied with natural graphite powder (15). A blend of concentrated sulfuric acid (150 ml), graphite (2.5 g), and $NaNO_3$ (1.5 g) within an ice bath were stirred for 40 min. Through severe stirring, $KMnO_4$ (9 g) was then added to the mixture. The speed of addition was intently controlled to hold the reaction temperature below 15ºC. Later, the mixture was stirred for two hours and transferred to ice bath to 30° C. Then, 250 mL of H_2O was

added. The reaction temperature which was enhanced to 95ºC was then steadied for 2 hours. In this stage, the mixed color gently turned brown. Afterward, 500 ml of water was added to the system. To reduce the remaining permanganate, 30 ml of H_2O_2 (30%) was also applied. At that time, the color mixture gently changed into yellow. The mixture was then washed and centrifuged to 6% HCl. Next, deionized water was added for many times until the pH became neutral. After the mixture was filtered and vacuum dried for 12 h, a solid and dry GO was achieved (16).

2.5. Batch adsorption experiments

For batch adsorption experiments solution, the initial concentration of IC was provided and pH of solution was adjusted with 1N sodium hydroxideor 1N hydrochloric acid solutions in the range of 2 to 8.After adding adsorbent to soluble, the samples were placed on shaker at 180 rpm for 15 min. After filtration, the absorption rate of each solute was computed by UV-visible spectrophotometer at λ_{max}= 645 nm and sorption efficiency (%), and the amount of IC adsorbed by Eqs. (1) and (2), respectively:

$$\text{Sorption efficiency (\%)} = \frac{C_0 - C_e}{C_0} \times 100 \quad (1)$$

$$q_e = \frac{(C_0 - C_e)\,V}{m} \quad (2)$$

Where Ce and C0 (mg/L) are the concentrations of IC at equilibrium and initially, respectively. qe (mg/g) is the amount of adsorbed IC at equilibrium, m is the weight of adsorbent (g), and V is the volume of the solution (L) (17). The Removal percentage of IC was also estimated by this Equation:

$$R(\%) = \frac{C_0 - C_e}{C_0} \times 100 \quad (3)$$

2.6. Error Analysis

For calculating the maximum stable isotherm and kinetic models in the experimental data, Chi-square test and Sum of Square Error (SSE%) were used:

$$SSE\% = \sqrt{((q_{e,exp} - q_{(e,cal)}/N)} \quad (4)$$

$$X^2 = (q_{(e,exp)} - q_{(e,cal)})^2 / q_{(e,cal)} \quad (5)$$

Where $q_{e,cal}$ and $q_{e,exp}$ are the values of the q_e predicted by the model, and experimental measured q_e and N is the number of $q_{e,exp}$ (18).

3. Result

3.1. Characterization of carbon nanostructures

The structures and morphologies of GO, AC, MWCNTs, and Oxidize –MWCNTs were observed with a SEM. The XRD was also measured by x-ray diffractometer. The SEM clearly showed the crystal tubular structure of nanotubes. The GO film was also lucid because of its irregular edge and single atom layered structure (Fig. 2A). The surface of Graphene oxide had lots of crumpling due to the navigation of GO sheets. The surface of AC was also documented to be very bristly and many pores were seen on it (Figure 2B). Pure MWCNTs was a hollow cylinder with random state and lengthy caliber (Figure 2C). Figure 1D clearly shows the crystalline tubular structure of oxidized MWCNTs.

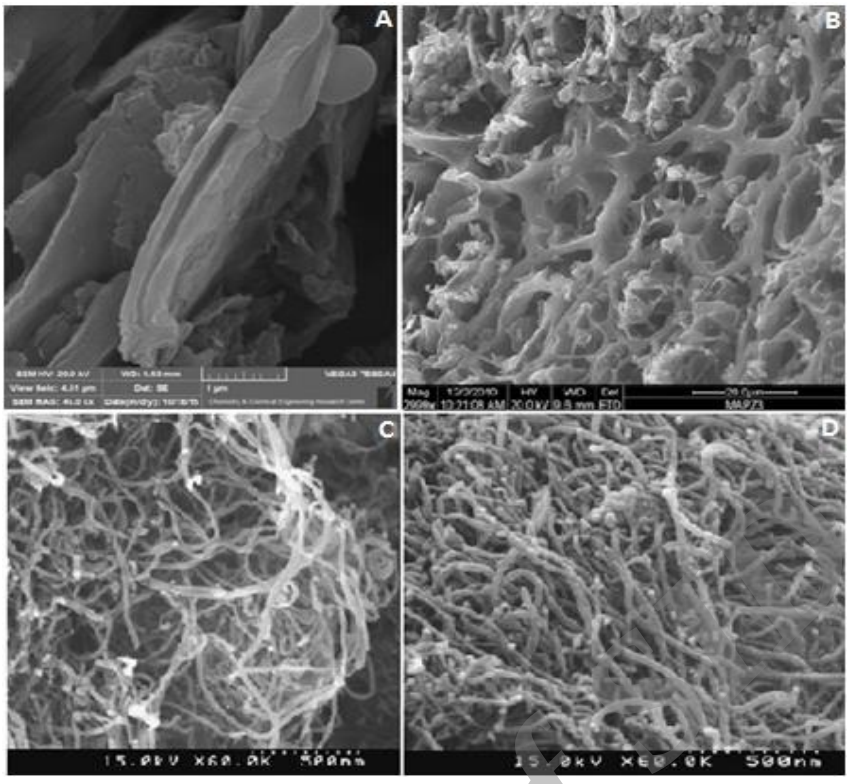

Figure 2. SEM images of (A) GO, (B) AC, (C) MWCNTs and (D) *Oxidize* –MWCNTs

The XRD characterization is used to provide information on the degree of nanotube alignment in addition to calculation on the amount of graphitization. The XRD of GO Nano-sheets are shown in Figure 3A. The diffraction peak corresponding to 2θ= 26.74 in the spectrum was related to 002 planes of Graphene oxide. The distances between layers of Graphene oxide may also be due to the existence of oxygen functional groups, such as carboxyl, hydroxyl, and epoxy. According to the results on XRD, it can be stated that graphite powder was fully oxidized. The form of diffraction background and the lack of sharp peak activated carbon showed an often amorphous structure in AC nature (Figure 3B). Diffraction background corresponding to 2θ=24.98° has also indicated 002 plane of AC structure (19). Figures 3C and 3D display the comparison between the XRD of the Oxidize MWCNTs and MWCNTs. The peak of the Oxidize MWCNTs display high severs peak at 2θ = 24.72°, and a low intense peak at 2θ=43.9°, corresponding to the (002) and (100) reflections, respectively. Additionally, the pattern of the MWCNTs indicated a high intense peak at 2θ=25.12°, and a low intense peak at 2θ =44.0°, respectively (20).

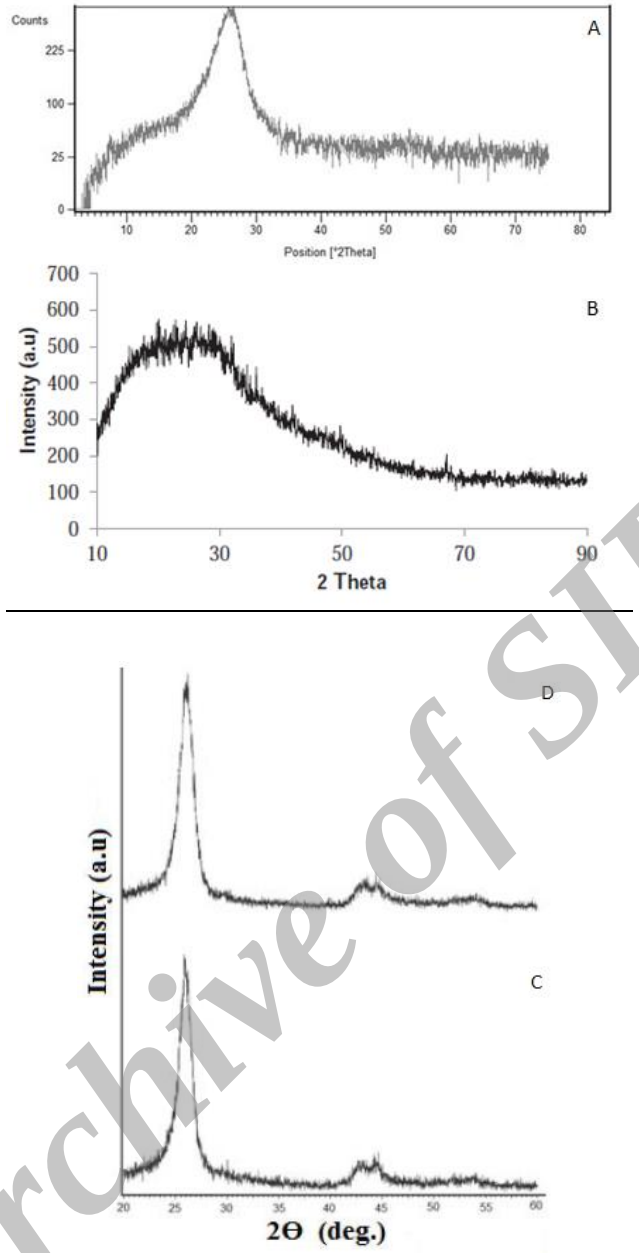

Figure 3. XRD patterns for (A) GO, (B) AC, (C) MWCNTs, and (D) *Oxidize* -MWCNTs

3.2. Effect of pH on the removal of dyes

The pH of the system to use deep penetration on the adsorptive nature of dye molecules, maybe due to its effect on the surface properties of the carbon nanostructures adsorbents and dissociation/ ionization of adsorbate molecule. The changes in removal of dye at different pH levels are presented in Figure4. As is shown there, the adsorption level of IC was enhanced by increasing the pH value of solution from 2.0 to 7.0. Both GO and Oxidized MWCNTs were observed to have very high removal efficiencies of 67.24–90.38% for GO and 61.81–88.49% for Oxidized MWCNTs, respectively. Also, the dye removal efficiency by AC and MWCNTs were found to be49.77-82.84% for AC and 53.31-82.58% for MWCNTs, respectively in the studied pH range.

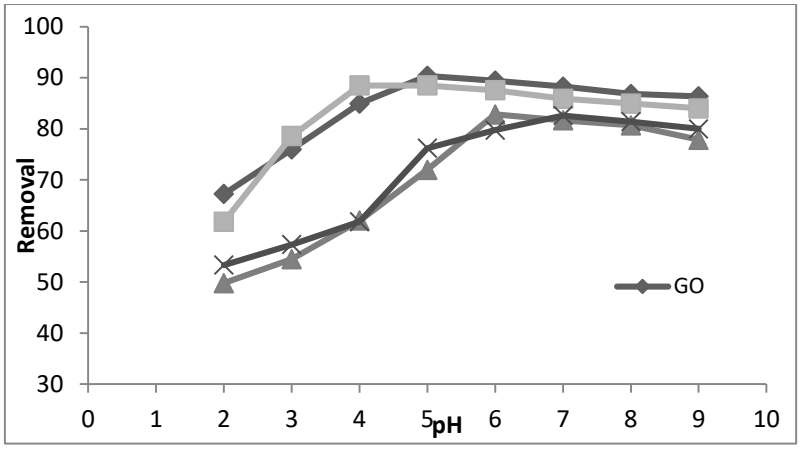

Figure 4. Effect of pH on IC adsorbed by GO, Oxidized MWCNTs, AC, and MWCNTs.

3.3. Effect of temperature on the removal of dyes

To investigate the effect of temperature, the adsorption experiments were performed at the range of 15–50ºC.The results are shown in Figure 5. The removal efficiencies for GO, Oxidized MWCNTs, AC, and MWCNTs were found to be94.39, 93.44, 89.19, and 88.01 which were achieved in 20ºC, 35ºC, 30ºC, and 35ºC temperatures, respectively. Thus, the adsorption capacity reduced with temperature increase. This reduction in the absorption rate with temperature increase may be due to the factors of weakening the forces of attraction between the enabled sites of the adsorbents, the kind of adsorbate, as well as the adjacent molecules of the adsorbed phases.

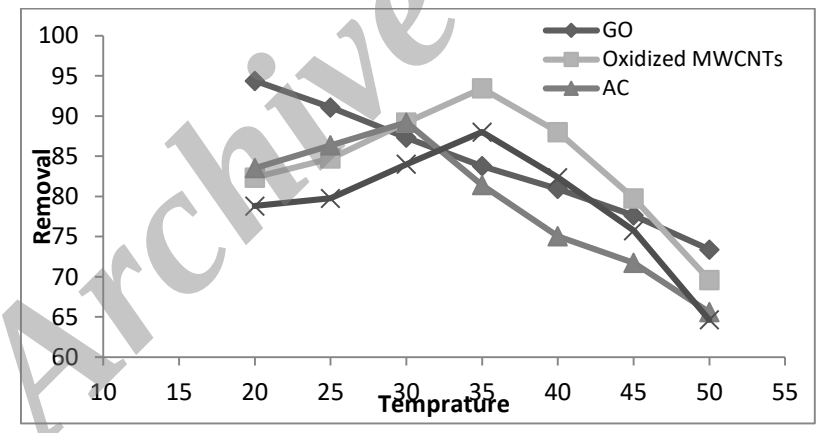

Figure 5. The effect of temperature on IC by GO, Oxidized MWCNTs, AC, and MWCN

3.4. Effect of concentration on the removal of dyes

In the present study, the kinetics of adsorption was investigated at different initial IC concentrations. The results indicated that the adsorption of IC molecules by GO, Oxidized MWCNTs, AC, and MWCNTs enhanced with any increase in concentration resulting in equilibrium values of about 12 mol/L, 10 mol/L, 15 mol/L, and 12 mol/L, respectively. The effect of concentration on the removal of IC is illustrated in Figure 6. The GO and Oxidized MWCNTs have seen to experience more removal ratesof93.44%, and 89.67% for GO and Oxidized MWCNTs, respectively (Figure7). Also the dye removal rate by AC and MWCNTs were found to be82.58% and 77.39% for AC and MWCNTs, respectively.

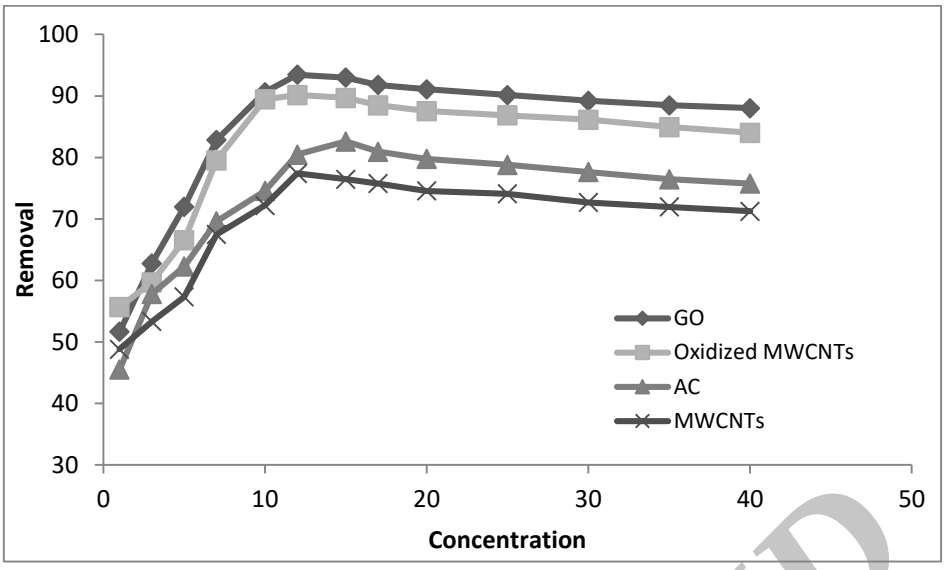

Figure 6. The effect of concentration on the IC by GO, Oxidized MWCNTs, AC and MWCN

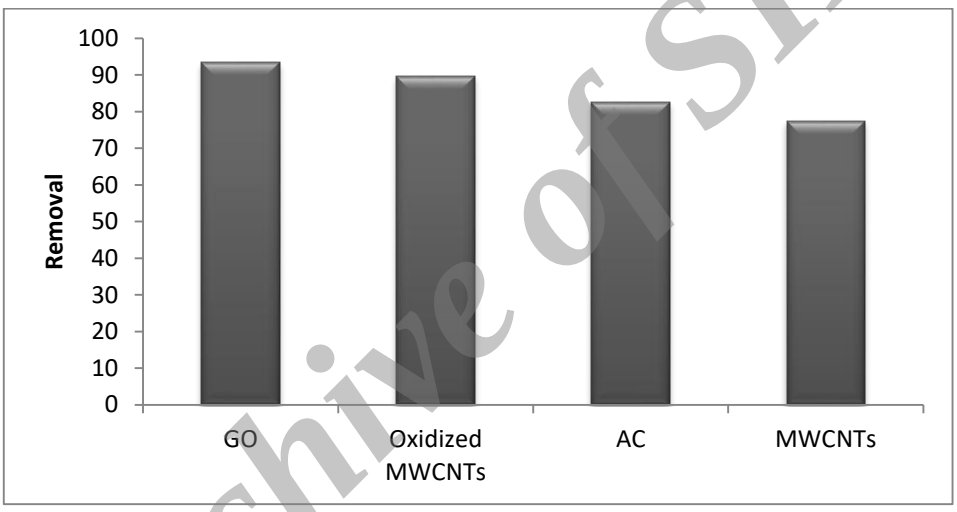

Figure 7. The effect of concentration on removal of IC by GO, Oxidized MWCNTs, AC and MWCN

3.5. Effect of Contact Time

The effect of contact time on the removal of IC dye by the four adsorbents in solution is shown in Figures 8 and 9. The results indicated that in all concentrations used, when the contact time between the four adsorbents and the dyes enhanced, the absorption rate was also increased. The maximum IC removal efficiencies were done in the 0-55 minute distance for GO, Oxidized MWCNTs, AC and MWCNTs. This could be due to the available number of vacant binding enabled sites for IC at the start of reaction and quantized coverage of the binding sites, which reduced the adsorption rate, until finally the equilibrium is achieved. In the residual concentration, the systems were nearly unchanged and not experiencing many adsorptions. Also, GO had high removal rate because of its individual atom layered structure for rapid absorption of IC molecules (24).

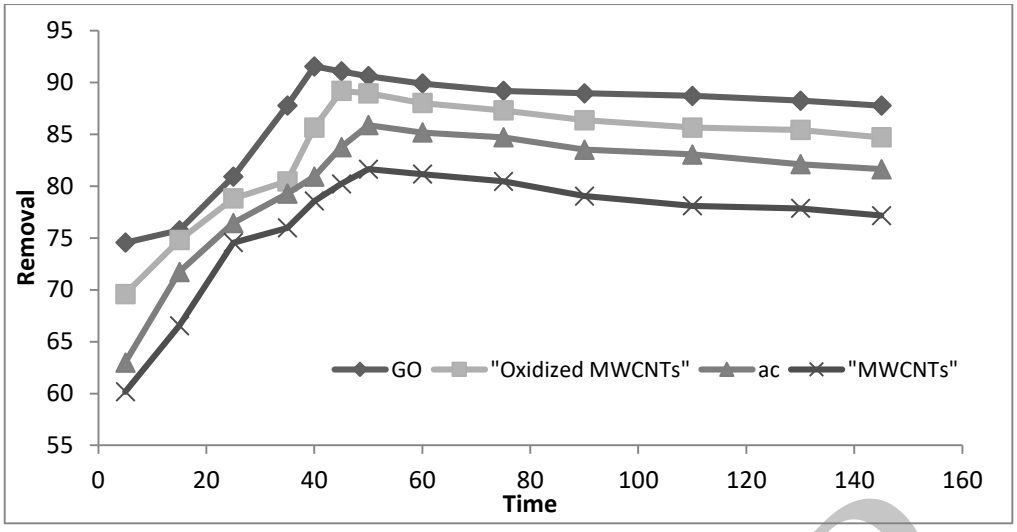

Figure 8. The effect of contact time on the IC by GO, Oxidized MWCNTs, AC and MWCN

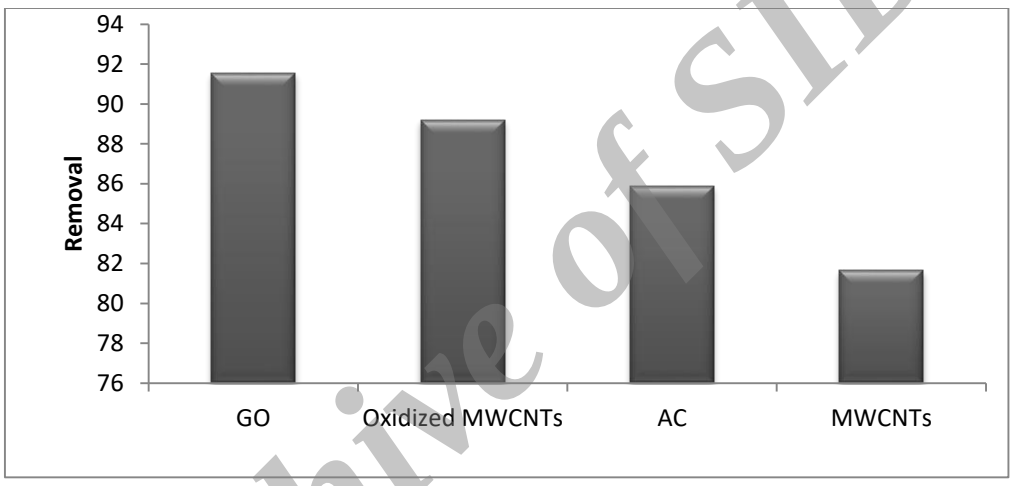

Figure 9. The effect of contact time on removal of IC by GO, Oxidized MWCNTs, AC and MWCN

4. Discussion

4.1. Adsorption isotherms

The adsorption isotherm is to provide certain relationship between the equilibrium concentration of adsorbate and the rate of adsorption on the surface. Langmuir adsorption model indicates that maximum adsorption corresponds to single layer of molecules on the surface of absorbent, without interaction with molecules to be absorbed. The Langmuir isotherm is hence applied in most single-layer adsorption methods. Langmuir Model is expressed by the following equation:

$$q_e = \frac{Q_0 b C_e}{1+bC_e} \quad (6)$$

The Langmuir equation can be explained in linear form:

$$\frac{C_e}{q_e} = \frac{C_e}{q_m} + \frac{1}{q_m b_1} \quad (7)$$

Where b1 is Langmuir constant (L/mg), C_e is IC concentration at equilibrium in solution (mg/l), q_m is IC concentration when single layer forms on adsorbent (mg/g), and qe is IC concentration at equilibrium onto one of carbon adsorbents (mg/g). The basic features of Langmuir isotherm can be displayed by the separation factor of RL that is expressed by the following equation (8):

$$R_L = \frac{1}{1+bC_0} \quad (8)$$

The RL value indicates the kind of isotherm that contains undesirable (R_L> 1), linear (R_L< 1), irreversible (R_L =0), or optimal sorption (0< R_L<1).The Freundlich isotherm can also be used as undesirable absorption on inhomogeneous surfaces and multilayer sorption. The Freundlich equation is presented as follows:

$$q_e = K_f C_e^{1/n} \quad (9)$$

Where, n is Freundlich constant, and KF is the Freundlich constant (L/mg). The values of n> 1 indicate an optimum absorption condition (25). To calculate the constants n and K_f, Freundlich equation can be used in a linear form:

$$\ln q_e = \frac{1}{n}\ln C_e + \ln K_f \quad (10)$$

Based on the findings, the removal efficiency of IC increased from 40.11 to 93.05% with any increase in adsorbent dose from 0.001 to 0.04 g, and the most adsorption rate was obtained at 0.04g (not shown in here).This could then be due to a rise in the surface area and having many enabled sites for adsorption. So, in this study, 0.02, 0.025, 0.03, and 0.025 g of GO, Oxidized MWCNTs, AC and MWCN were respectively selected as adsorbent dose due to the acceptable sorption capacity and higher sorption efficiency. Checking the equilibrium data was very useful for assessing the adsorption properties of GO, Oxidized MWCNTs, AC and MWCNTs adsorbents. Figure 10 shows that the adsorption isotherm experiments of IC onto four adsorbents were fitted to Langmuir and Freundlich models.

The results further showed that the removal efficiency changed related to the type of adsorbent and dye used. It was also observed that the correlation coefficient values calculated from the Langmuir isotherm model is more appropriate to characterize IC adsorption onto adsorbents. The related parameters are evaluated and listed in Table 1. According to the table, RL value was in the range of 0-1 suggesting that the IC molecules adsorbed on the adsorbent under the conditions used in this study was desirable. In the Langmuir isotherm model it is assumed that the single layer adsorptions are on the adsorbent surface with the same finite number of sites while all sites had equivalent energy. According to the results, the adsorption of IC by the four adsorbents was done in a single layer adsorption. At the same time, Freundlich constant (n) depended on the severity of adsorption and the values of n>1 indicated that the adsorption process was desirable. As is shown in Table 1, the evaluated value of n>1 was obtained, which showed that under the conditions used in this study, the adsorption of IC molecules on adsorbents is desirable. The results demonstrated that Langmuir isotherm and pseudo-second-order Model are better than pseudo-first-order and in agreement with those reported in the literature (19, 23).

Table 1. Isotherm parameters of adsorption of IC onto four adsorbents

Adsorbent	Langmuir				Freeundlich		
	b	q_m	R_L	R^2	K_F	n	R^2
GO	50.00	0.013	0.286	0.994	150.64	4.97	0.945
OMWCNTs	37.04	0.016	0.351	0.994	129.85	4.40	0.937
AC	11.12	0.024	0.645	0.984	148.09	2.81	0.951
MWCNTs	12.34	0.020	0.618	0.987	132.82	2.52	0.950

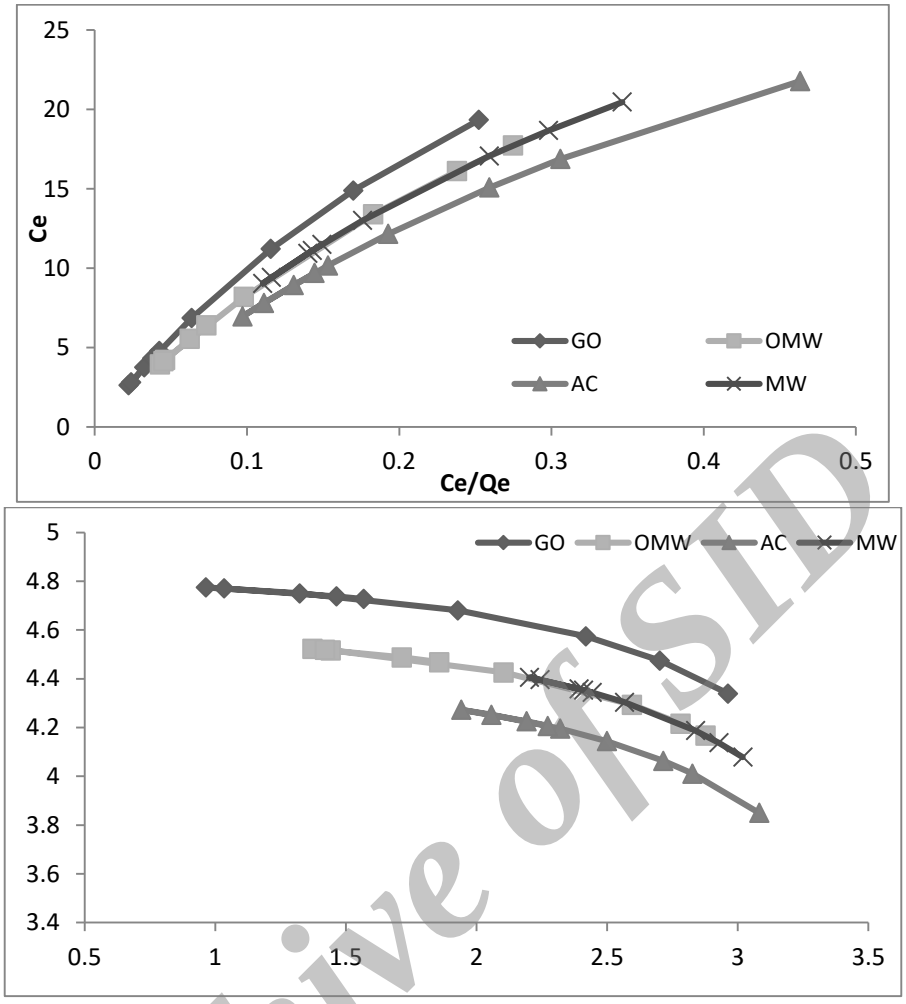

Figure 10. (a) Langmuir and (b) Freundlich isotherms for the adsorption of IC onto GO, Oxidized MWCNTs, AC and MWCNTs

4.2. Sorption kinetics

In order to analyze the kinetic data, the first-order and pseudo-second-order kinetic models were used. The Lagergren's equation for the first order kinetics is presented as follows:

$$\ln(q_e - q_t) = \frac{\ln q_e - k_1 t}{2.303} \quad (11)$$

Where qt (mg/g) is the amount of adsorbate adsorbed and $k_1(min^{-1})$ is the rate constant. The qe and k1 are computed from the slope and intercept of the plot which are listed in Table 2.The results indicated that the first-order model did not fit well. It was also observed that the q_e Cal values did not agree with the qe exp values. This indicated that the absorption of the absorbent IC in lower concentrations did not follow the first-order kinetics. It was also revealed that the absorption ofIC on carbon adsorbate did not follow this model. Pseudo-second-order model is given as follows(25):

$$\frac{t}{q_t} = \frac{1}{k_2 q_e^2} + \frac{t}{q_e} \quad (12)$$

Where the k_2 (g/mg min) second-order constant and (qe) the equilibrium sorption capacity can be calculated from the intercept and slope of plot t/qt versus t (Figure 11). Commonly, at lower dye concentrations, the adsorption rate was faster. Although, at each studied concentration, the correlation coefficient was higher for GO than other adsorbents. The results also indicated that the experimental values (qe(exp)) for the adsorption capacities well fitted with calculated values (qe(cal)), implying that the pseudo-second-order model was appropriate for IC adsorption kinetics by the GO, Oxidized MWCNTs, AC and MWCNTs (Figure 11). At the same time, the low rate of constant (k_2) suggested that adsorption rate was reduced by enhancing in time, which corresponded to the number of unoccupied sites provided in Table 2. Thus, the electrostatic attraction helped in IC being adsorbed by AC, GO, and MWCNTs. With a number of aforesaid privileges, such as great sorption capacity, stronger chemical-nanotub interactions and fast equilibrium rates, Oxidized MWCNTs were raised as premier sorbents for inorganic pollutant and organic chemicals than the AC (26). The findings of the current research were found to be in line with the results of a study carried out by Zhang et al. on water treatment using oxidized MWCNTs, and a study carried out by Ghaedi et al. on alizarin red S and more in removal using Multiwalled carbon nanotubes(6, 7). Also, the results of this study were observed to be consistent with the results of a research conducted by Yang et al. on the adsorption of Ni (II) on oxidized multi-walled carbon nanotubes (10).

Table2. First-order and pseudo-second-order kinetic model parameters for the adsorption of IC molecules onto GO, Oxidized MWCNTs, AC and MWCNTs

		First-order model					**Pseudo-second-order model**				
	q_{eexp}	q_{eCal}	K_1	SSE%	X^2	R^2	q_{eCal}	K_2	SSE%	X^2	R^2
GO	116.6	34.98	0.025	2.72	190.44	0.370	118.0	0.032	0.36	0.017	0.997
OMWCNTs	91.4	29.31	0.018	2.27	131.53	0.295	90.9	0.030	0.20	0.003	0.997
AC	73.9	25.37	0.023	2.01	92.83	0.330	76.9	0.024	0.52	0.117	0.991
MWCNTs	85.3	24.86	0.018	2.24	146.94	0.222	83.3	0.144	0.41	0.048	0.986

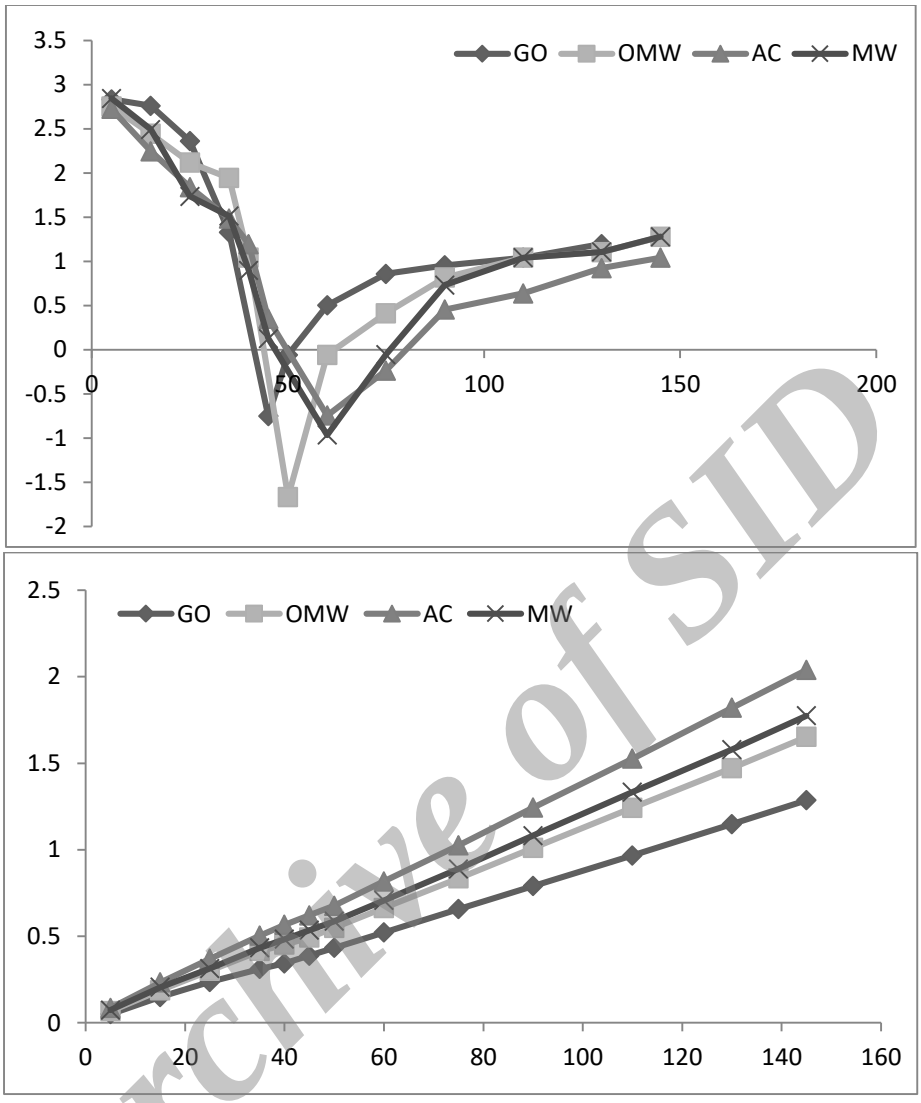

Figure 11. (a) First-order kinetic and (b) pseudo-second-order kinetic plot for the adsorption of IC onto GO, Oxidized MWCNTs, AC and MWCNTs

4.3. Error Analysis

In this research, the statistical analysis methods, such as correlation coefficient (R^2), Chi-square test (X^2), and sum of square error (SSE%) were applied to examine the fitness of various models to the achieved experimental data and determine the premier model for predicting the adsorption process, the results of which are shown in Table 2 and Figure 12. According to the results, the pseudo-second-order model had the best fit and higher R^2 and lower X^2. Also, SSE% for grapheme oxide indicated that its precision was better than the other three adsorbents.

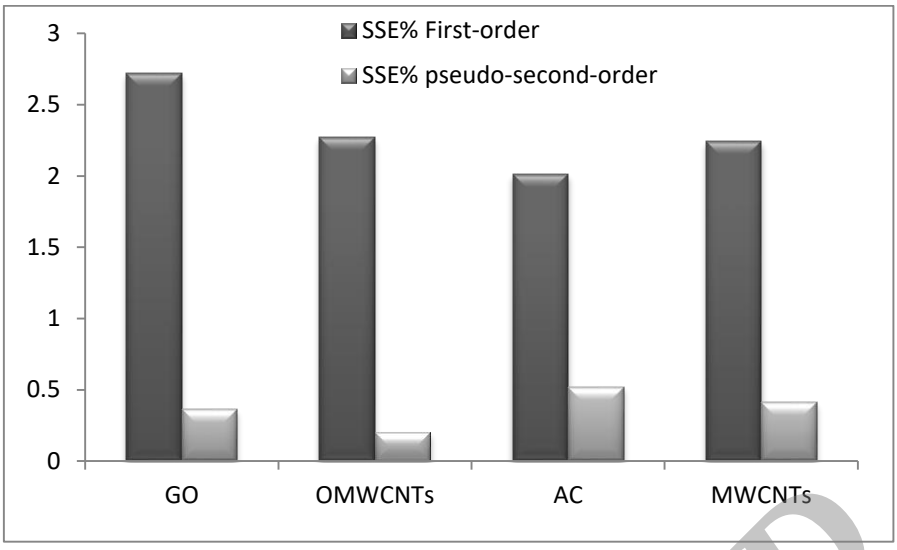

Figure 12. Comparison of different kinetic model precisions

4. Conclusion

Four carbon nanostructures, such as the GO, Oxidized MWCNTs, AC, and MWCNTs were studied for IC removal from aqueous solutions. The adsorbents represented a porous structure and well-developed surface that was useful for treating wastewater contaminated dye. Four carbon nanostructures adsorbents displayed a high adsorptive capacity for IC under the conditions used in this research. The results also indicated better efficiency for GO in IC removal than other carbon adsorbents. Furthermore, the isotherm parameters for the Freundlich and Langmuir models were calculated. The kinetics research demonstrated that the experimental data was good fitted by pseudo-second-order equation.

Acknowledgements

The authors would like to thank Ilam University for providing support for the present project. This article is derived from the PhD dissertation code 654.

Conflict of interest

No potential conflict of interest relevant to this article was reported.

References

1. Swaminathan S, Muthumanickkam A, Imayathamizhan NM. An effective removal of methylene blue dye using polyacrylonitrile yarn waste/graphene oxide nanofibrous composite, International Journal of Environmental Science and Technology. 2015; 12(11):3499–3508. https://doi.org/10.1007/s13762-014-0711-z
2. Shi H, Li W, Zhong L, Xu C. Methylene Blue Adsorption from Aqueous Solution by Magnetic Cellulose/Graphene Oxide Composite: Equilibrium, Kinetics, and Thermodynamics. Industrial & Engineering Chemistry Research. 2014; 53(3): 1108-1118. DOI**:** 10.1021/ie4027154
3. Yenikaya C, Atar E, Olgun A, Atar N, Ilhan S, Colak F. Biosorption Study of Anionic Dyes from Aqueous Solutions using Bacillus Amyloliquefaciens, Engineering in Life Sciences. 2010; 10: 233 –241. DOI: 10.1002/elsc.200900108
4. Nassar MM, El-Geundi MS, Al-Wahbi AA. Equilibrium modeling andThermodynamic Parameters for Adsorption of Cationic Dyes onto Yemen NaturalClay, Desalination and Water Treatment. 2012; 44(1-3):340-349. http://dx.doi.org/10.1080/19443994.2012.691701
5. Prola LT, Machado FM, Bergmann CP, de Souza FE, Gally CR, Lima EC, AdebayoMA., Dias SLP, Calvete T. Adsorption of Direct Blue 53 Dye from

Aqueous Solutions by Multi-Walled Carbon Nanotubes and Activated Carbon, Journal of Environmental Management. 2013; 130: 166-175. doi: 10.1016/j. jenvman. 2013. 09.003.
6. Ghaedi M, Kokhdan SN. Oxidized multiwalled carbon nanotubes for the removal of methyl red (MR): kinetics and equilibrium study, Desalintion Water Treatatment. 2012; 49(1-3): 317–325. http://dx.doi.org/10.1080/19443994.2012.719355
7. Zhang H, Lin G, Zhou Z, Dong X, Chen T. Raman spectra of MWCNTs and MWCNT-based H2 adsorbing system, Carbon. 2002; 40 (13): 2429–2436.https:// doi. org/ 10. 1016/S0008-6223(02)00148-3
8. Jayanthi S, Eswar NKR, Singh SA, Chatterjee K, Madras G, Sood AK. Macroporous three-dimensional graphene oxide foams for dye adsorption and antibacterial applications, RSC Advances. 2016; 6: 1231-1242. DOI: 10.1039/ C5RA19925E
9. Ska P. Carbon nanotubes as sorbents in the analysis of pesticides. Chemosphere. 2011; 83(11):1407–1413.https:// doi.org/ 10. 1016/j. chemosphere.2011.01.057
10. Yang S, Li J, Shao D, HuJ, Wang X. Adsorption of Ni (II) on oxidized multi-walled carbon nanotubes: effect of contact time, pH, foreign ions and PAA. Journal of Hazardous Materials. 2009; 166: 109–116.https://doi.org/10.1016/j.jhazmat.2008.11.003
11. Mauter MS, Elimelech M. Environmental applications of carbon-based nanomaterials. Environmental Science & Technology. 2008; 42(16):5843–5859. DOI: 10.1021/es8006904
12. Muataz AT, Omer YB, Bassam AT, Alaadin B, FarajAB, Mohamed F. Effect of carboxylic group functionalized on carbon nanotubes surface on the of lead from water. Bioinorganic Chemistry and Applications. 2010; 8:1–9. http://dx.doi.org/10. 1155/ 2010/603978
13. Brunauer S, Emmett PH. removal. & Teller, E. Adsorption of gases in multimolecular layers. Journal of the American Chemical Society. 1938; 60 (2):309–319.DOI: 10.1021/ja01269a023.
14. Teng HS, Yeh TS, Hsu LY. Preparation of activated carbon from bituminous coal with phosphoric acid activation. Carbon. 1998; 36(9): 1387–1395.https://doi. org/10. 1016/ S0008-6223(98)00127-4
15. Agorku ES, Mamo MA, Mamba BB, PandeyAC, Mishra AK. Cobalt-doped ZnS-reduced graphene oxide nanocompositeas an advanced photo catalytic material. Journal of Porous Materials. 2015; 22 (1):47–56. doi: 10.1007/s10934-014-9871-y
16. Woan K, Pyrgiotakis G, Sigmund W. Photocatalytic carbon-nanotube-TiO2 composites. Advanced Materials. 2009; 21(21):2233–2239. DOI: 10.1002/ adma. 200802738
17. Safarik I, Angelova R, Baldikova E, Pospiskova K, Safarikova M.Leptothrix sp. sheaths modified with iron oxide particles: Magnetically responsive, high aspect ratio functional material, Materials Science and Engineering: C. 2017; 71: 1342-1346. DOI: 10.1016/j.msec.2016.10.056
18. Han R, Wang Y, Han P, Shi J, Yang J, Lu Y. Removal of methylene blue from aqueous solution by chaff in batch mode. Journal of Hazardous Materials. 2006; 137(1): 550-57.https://doi.org/10.1016/j.jhazmat.2006.02.029
19. Chen Y, Chen W, Huang B, Huang M. Process optimization of K2 C2O4 -activated carbon from kenaf core using Box – Behnken design. Chemical Engineering Research and Design. 2013; 91(9):1783-1789. https://doi.org/10.1016/j.cherd.2013.02.024
20. Zhang L, Li X, Wang M, He Y, Chai L, Huang J, Wang H, Wu X, Lai Y. Highly Flexible and Porous Nanoparticle-Loaded Films for Dye Removal by Graphene Oxide–Fungus Interaction, ACS Applied Materials & Interfaces. 2016; 8(50): 34638–34647. doi: 10.1021/acsami.6b10920.
21. Yang ST, Chen S, Chang Y, Cao A, Liu Y, Wang H. Removal of methylene blue from aqueous solution by graphene oxide. Journal of Colloid and Interface Science. 2011; 359(1): 24–29.https://doi. org/10.1016/ j.jcis.2011.02.064
22. Zuccaro L, Krieg J, Desideri A, Kern K, Alasubramanian K. Tuning the isoelectric point of graphene by electrochemical functionalization, Scientific Reports. 2015; 5: 11794-11801. DOI: 10.1038/srep11794
23. Szlachta M, Wójtowicz P. Adsorption of methylene blue and Congo red from aqueous solution by activated carbon and carbon nanotubes, Water Science &

Technology. 2013; 68(10):2240-2248. doi: 10.2166/wst.2013.487.

24. Wu T, Cai X, TanS, Li H, Liu J, Yang W. Adsorption characteristics of acrylonitrile, p-toluenesulfonic acid, 1-naphthalenesulfonic acid and methyl blue on graphene in aqueous solutionsChemical Engineering Journal. 2011; 173(1):144–149.https://doi.org/10.1016/j.cej.2011.07.050
25. Papaevangelou VA, Gikas GD, Tsihrintzis VA Chromium removal from wastewater using HSF and VF pilot-scale constructed wetlands: Overall performance, and fate and distribution of this element within the wetland environment, Chemosphere. 2017; 168: 716-730. doi: 10.1016/j. chemosphere. 2016.11.002.
26. Wu WH, Chen W, Lin DH, Yang K. Influence of surface oxidation of multiwalled carbon nanotubes on the adsorption affinity and capacity of polar and nonpolar organic compounds in aqueous phase. Environmental Science & Technology. 2012; 46(10): 5446-5454.DOI: 10.